Supporting Information

Counterflow Gradient Focusing in Free-Flow Electrophoresis for Protein Fractionation

Matthew Courtney,‡ Ethan Thompson,† Tomasz Glawdel, ‡ Carolyn L. Ren*,‡

†Department of Nanotechnology Engineering, University of Waterloo, 200 University Avenue West, Waterloo, Canada
‡Department of Mechanical and Mechatronics Engineering, University of Waterloo, 200 University Avenue West, Waterloo, Canada

***Corresponding Author:** c3ren@uwaterloo.ca

Table of Contents

The following Table S1 provides a list of the symbols used throughout the derivation of the FF-CGF mathematical model that can be used as a reference for Sections 1, 2, and 3:

Table S1: Summary of Mathematical Symbols

x	Position in the *x*-direction.
y	Position in the *y*-direction.
z	Position in the *x*-direction.
L	Length of the separation chamber.
$2b$	Breadth of the separation chamber.
$2h$	Height of the separation chamber.
$\dot{V}$	Volumetric flow rate through an arbitrary segment of the separation chamber.
Δx	Width of abritrary segment in the separation chamber that is much smaller than the breadth, $2b$.
Δz	Length of abritrary segment in the separation chamber that is much smaller than the length, L.
$\langle u \rangle$	Area-averaged *x*-velocity of the fluid flow.
$\langle w \rangle$	Area-averaged *z*-velocity of the fluid flow.
u_0	Area-averaged *x*-velocity of the fluid flow at the left sidewall of the FFE chamber ($x = -b$).
u_1	Area-averaged *x*-velocity of the fluid flow at the right sidewall of the FFE chamber ($x = b$).
$\langle w \rangle_0$	Area-averaged *z*-velocity of the fluid flow at the beginning of the chamber ($z = 0$).
$\nabla\langle u \rangle$	The slope of the counterflow velocity gradient in a symmetric gradient ($\nabla\langle u \rangle = u_0/b$).
u_{EP}	Electrophoretic velocity of an analyte.
μ_{EP}	Electrophoretic mobility of an analyte.
E	Electric field applied across the FFE chamber.
u_{T}	Total analyte velocity in the *x*-direction.
t	The amount of time for a given analyte in the FFE chamber.
$\langle x \rangle_f$	Area-averaged focal point for a given analyte in the *x*-velocity.
u	The *x*-velocity of the fluid flow.
w	The *z*-velocity of the fluid flow.
x_f	The shifted focal point for a given analyte in the *x*-direction.

Section 1: Counterflow Gradient

A simplified 2D mathematical model of the velocity field within the FF-CGF chamber can be derived using a method similar to Ref. [S1]. This model will solve for the area-averaged x-velocity $\langle u \rangle$ and area-averaged z-velocity $\langle w \rangle$. For this model, consider a chamber where the length L and breadth $2b$ are much greater than the height $2h$ (see Fig. S1a). By assuming incompressible flow, the net volumetric flow rate $\dot{V}$ through an arbitrary segment of the chamber with a width of Δx and a length of Δz is equal to zero (see Fig. S1b):

$$\dot{V} = 2h\Delta z(\langle u \rangle_x - \langle u \rangle_{x+\Delta x}) + 2h\Delta x(\langle w \rangle_z - \langle w \rangle_{z+\Delta z}) = 0 \tag{S1}$$

If the segment being analyzed is much smaller than the length and the breadth of the chamber, then the following expressions can be written:

$$\langle u \rangle_{x+\Delta x} - \langle u \rangle_x = \frac{d\langle u \rangle}{dx}\Delta x \tag{S2}$$

$$\langle w \rangle_{z+\Delta z} - \langle w \rangle_z = \frac{d\langle w \rangle}{dz}\Delta z \tag{S3}$$

By substituting these equations back into Eq. (S1), the following expression can be obtained:

$$\frac{d\langle u \rangle}{dx} + \frac{d\langle w \rangle}{dz} = 0 \tag{S4}$$

If the inflow through the sidewalls is assumed to be constant along the z-direction and described by mean velocities u_0 and u_1, then Eq. (S4) can be simplified by setting Δx of the segment equal to breadth of the chamber $2b$:

$$\frac{d\langle w \rangle}{dz} = \frac{u_0 - u_1}{2b} \tag{S5}$$

Solving for $\langle w \rangle$ in Eq. (S5) gives the following expression:

$$\langle w \rangle = \left(\frac{u_0 - u_1}{2b}\right)z + \langle w \rangle_0 \tag{S6}$$

Additionally, substituting Eq. (S5) back into Eq. (S4) gives the following expression:

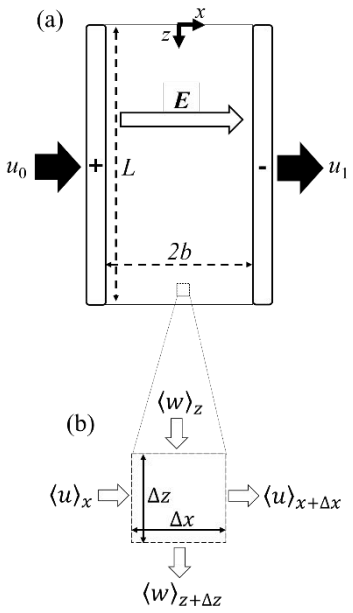

Figure S1. (a) A 2D FF-CGF chamber used for the mathematical model. (b) An enlarged segment of the chamber.

$$\frac{d\langle u \rangle}{dx} = -\left(\frac{u_0 - u_1}{2b}\right) \tag{S7}$$

Solving for $\langle u \rangle$ in Eq. (S7) gives the following expression:

$$\langle u \rangle = -\left(\frac{u_0 - u_1}{2b}\right)x + \langle u \rangle_0 \tag{S8}$$

By applying the boundary conditions of $\langle u \rangle = u_0$ at $x = -b$ and $\langle u \rangle = u_1$ at $x = b$, the final expression for $\langle u \rangle$ is:

$$\langle u \rangle = \left(\frac{u_0 + u_1}{2}\right) - \left(\frac{u_0 - u_1}{2b}\right)x \tag{S9}$$

For the scenario where $u_0 = -u_1$, the expressions for $\langle u \rangle$ and $\langle w \rangle$ are:

$$\langle u \rangle = -\frac{u_0}{b}x = -\nabla\langle u \rangle\, x \tag{S10}$$

$$\langle w \rangle = \frac{u_0}{b}z + \langle w \rangle_0 = \nabla\langle u \rangle\, z + \langle w \rangle_0 \tag{S11}$$

Section 2: Position and Residence Time

The average-area velocity field within the chamber can be used to track the position of the analyte at time t. Substituting Eq. (S10) into Eq. (2), the x-velocity of a mass particle with a constant u_{EP} can be determined from the following expression:

$$\frac{\partial\langle x\rangle}{\partial t} = u_{\mathrm{EP}} - \nabla\langle u\rangle\, x \tag{S12}$$

Assuming $x = 0$ at $t = 0$, this differential equation can be used to find the mean x-position of the analytes as a function of t:

$$\langle x\rangle = \frac{u_{\mathrm{EP}}}{\nabla\langle u\rangle}\left(1 - e^{-\nabla\langle u\rangle\, t}\right) \tag{S13}$$

Now, rewriting Eq. (S11) to consider the z-velocity of a mass particle:

$$\frac{\partial\langle z\rangle}{\partial t} = \nabla\langle u\rangle\, z + \langle w\rangle_0 \tag{S14}$$

Assuming $z = 0$ at $t = 0$, this differential equation can be used to find the mean z-position of the analytes as a function of t:

$$\langle z\rangle = \frac{\langle w\rangle_0}{\nabla\langle u\rangle}\left(e^{\nabla\langle u\rangle\, t} - 1\right) \tag{S15}$$

Rearranging this equation to solve for t gives:

$$t = \frac{1}{\nabla\langle u\rangle} ln\left(1 + \frac{\nabla\langle u\rangle}{\langle w\rangle_0}\langle z\rangle\right) \tag{S16}$$

Setting $\langle z\rangle = L$ into this equation will give the residence time of the analyte in the separation chamber. Substituting this expression back into Eq. (S13) gives the mean x-position of an analyte with a constant u_{EP} as a function of $\langle z\rangle$:

$$\langle x\rangle = \frac{u_{\mathrm{EP}}}{\nabla\langle u\rangle}\left(1 - \left(1 + \frac{\nabla\langle u\rangle}{\langle w\rangle_0}\langle z\rangle\right)^{-1}\right) \tag{S17}$$

A graphical representation of Eq. (S17) in Fig. S2 shows the mean x-position of different analytes in a 2D chamber with a given x-velocity gradient.

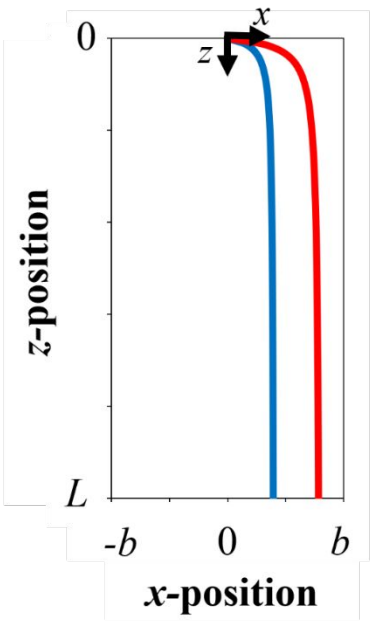

Figure S2. (a) Tracking the *x*-position of analytes with different mobilities as they move along the *z*-direction.

Section 3: Focal Point

The mean focal point for an analyte with a constant u_{EP} can also be found using the average-area velocity field in the chamber. Substituting Eq. (S10) into Eq. (2) gives the following expression:

$$u_T = u_{EP} - \nabla\langle u\rangle\, x \tag{S18}$$

Analytes will migrate towards its focal point (where u_T crosses the *x*-axis), regardless of its initial *x*-position. Therefore, at $u_T = 0$, the mean focal point is:

$$\langle x\rangle_f = \frac{u_{EP}}{\nabla\langle u\rangle} \tag{S19}$$

When considering the overall focal point x_f of an analyte, it is also important to consider velocity profile of the fluid flow in the height direction of the chamber (*y*-direction). If it is assumed that the *x*-velocity (u) and the *z*-velocity (w) of the fluid within the chamber are constrained to a parabolic profile in the *y*-direction:

$$u(y) = \frac{3}{2}\langle u\rangle\left(1 - \frac{y^2}{h^2}\right) \tag{S20}$$

$$w(y) = \frac{3}{2}\langle w\rangle\left(1 - \frac{y^2}{h^2}\right) \tag{S21}$$

Substituting Eq. (S10) and Eq. (S11) into Eq. (S20) and Eq. (S21), respectively, then the overall velocity profiles are given as:

$$u(x,y) = \ -\frac{3}{2}\nabla\langle u\rangle\, x\left(1 - \frac{y^2}{h^2}\right) \tag{S22}$$

$$w(y,z) = \frac{3}{2}(\nabla\langle u\rangle\, z \ + \ \langle w\rangle_0)\left(1 - \frac{y^2}{h^2}\right) \tag{S23}$$

From Eq. (S22), if $u_{\mathrm{EP}} = \ -u(x,y)$ at the focal point, and a shifted co-ordinate of $x = \langle x\rangle_f + x_f$ is applied, then the focal point is given by:

$$x_f \ = \frac{u_{\mathrm{EP}}}{\nabla\langle u\rangle}\left(\frac{2}{3}\left(1 - \frac{y^2}{h^2}\right)^{-1} - 1\right) \tag{S24}$$

Section 4: Numerical Simulations

To demonstrate the FF-CGF principle, a simplified 2D simulation for the proposed FFE chamber seen in Fig. 1a (COMSOL v5.3). The model used for this study is similar to a previously developed FF-IEF model [S2]. The fluid dynamics were calculated using the continuity equation and a simplified Navier-Stokes equation that neglected the inertial terms and the electrokinetic body forces:

$$\nabla \cdot \vec{\mathbf{u}} = 0 \tag{S25}$$

$$-\nabla p + \ \mu\nabla^2\vec{\mathbf{u}} - 12\frac{\mu\vec{\mathbf{u}}}{d_y^2} = 0 \tag{S26}$$

where $\vec{\mathbf{u}}$ is the velocity of the fluid, p is the hydrostatic pressure, and μ is the dynamic viscosity. Also note that the final term in Eq. (S26) is due to the shallow channel height approximation, with d_y being the chamber height. The electrostatics were computed simultaneously using the following equation:

$$\vec{E} = \ -\nabla V \tag{S27}$$

where $\vec{E}$ is the electric field and V is the electric potential. The chamber dimensions are 15 mm x 35 mm x 0.1 mm. There is a 0.5 mm wide sample inlet centered at the top of the chamber. The outlet is located at the bottom of the chamber with an exit pressure of 0 Pa. The fluid velocity within the chamber when the input velocity is 1 mm/s at both sidewalls and at the sample inlet.

The steady-state analyte transport through the chamber was then calculated using the convection-diffusion equation and the molar flux (N_i) equation:

$$\nabla \cdot \left(- D_i \nabla c_i + \mu_{EP} c_i \vec{E} \right) + \vec{\mathbf{u}} \cdot \nabla c_i = 0 \tag{S28}$$

$$- D_i \nabla c_i + \left(\vec{\mathbf{u}} + \mu_{EP} \vec{E} \right) c_i = N_i \tag{S29}$$

where D_i is the diffusion coefficient of the i^{th} analyte and c_i is the molar concentration of that analyte. The diffusive term that helps determine the width of the focused band only accounts for molecular diffusion in this model. Three analytes are injected at the sample inlet, each with a concentration of 1 mol/m^3. The COMSOL inputs for the diffusion coefficients for all three analytes was 10^{-10} m^2/s, while their mobilities were 0, 1×10^{-13}, and 2×10^{-13} s·mol/kg.

Section 5: Device Design

To reduce the concept of FF-CGF to practice a design of the FFE chamber was critical to replicate the hydrodynamic and electric field distribution in the simplified simulation. Our approach was to have parallel microchannels that connect to the sidewalls and span the entire length of the separation chamber (see Fig. S3a). At the other end of the microchannels, we placed additional side chambers that included access holes for buffer inflow and electrodes. There were also outlet channels placed between the end of the separation chamber and the outlets to ensure that the outlets did not affect the sample streamlines. For a uniform velocity gradient and electric field across the separation chamber, there must be an equal buffer flow rate (Q) and electrical current (I) through all of the microchannels. For this to be the case, the hydrodynamic resistance (R_H) and electrical resistance (R_E) of the microchannels (R_1) must be significantly greater than that of the side chambers (R_2) and the separation chamber (R_3).

To better understand this concept, the microfluidic network of the FFE device can be approximated as a circuit (see Fig. S3b). Different regions of the microfluidic network are considered to be resistors, where the pressure drop (ΔP) and the voltage drop (ΔV) across these resistors are defined as $\Delta P = QR_H$ and $\Delta V = IR_E$, respectively [S3]. A simplified version of this circuit is shown in Fig. 6b that divides the device into upper, middle, and lower sections. For the fluid mechanics, using the Kirchhoff's law analogy [S3], if $R_1 \simeq R_2 \simeq R_3$, ΔP from the side chamber to the outlet will be different for all three sections, and therefore Q through the microchannels will be inconsistent. However, if $R_1 >> R_2 \simeq R_3$, ΔP from the side chamber to the outlet will be comparable for all three sections, and therefore Q will be approximately uniform through all microchannels. The same assumption can be made for ΔV through the microfluidic network, except the position of the electrodes is considered instead of the inlets and outlets.

Decreasing the height (h) of the microchannels relative to the chambers can increase their R_H and R_E due to the following equations:

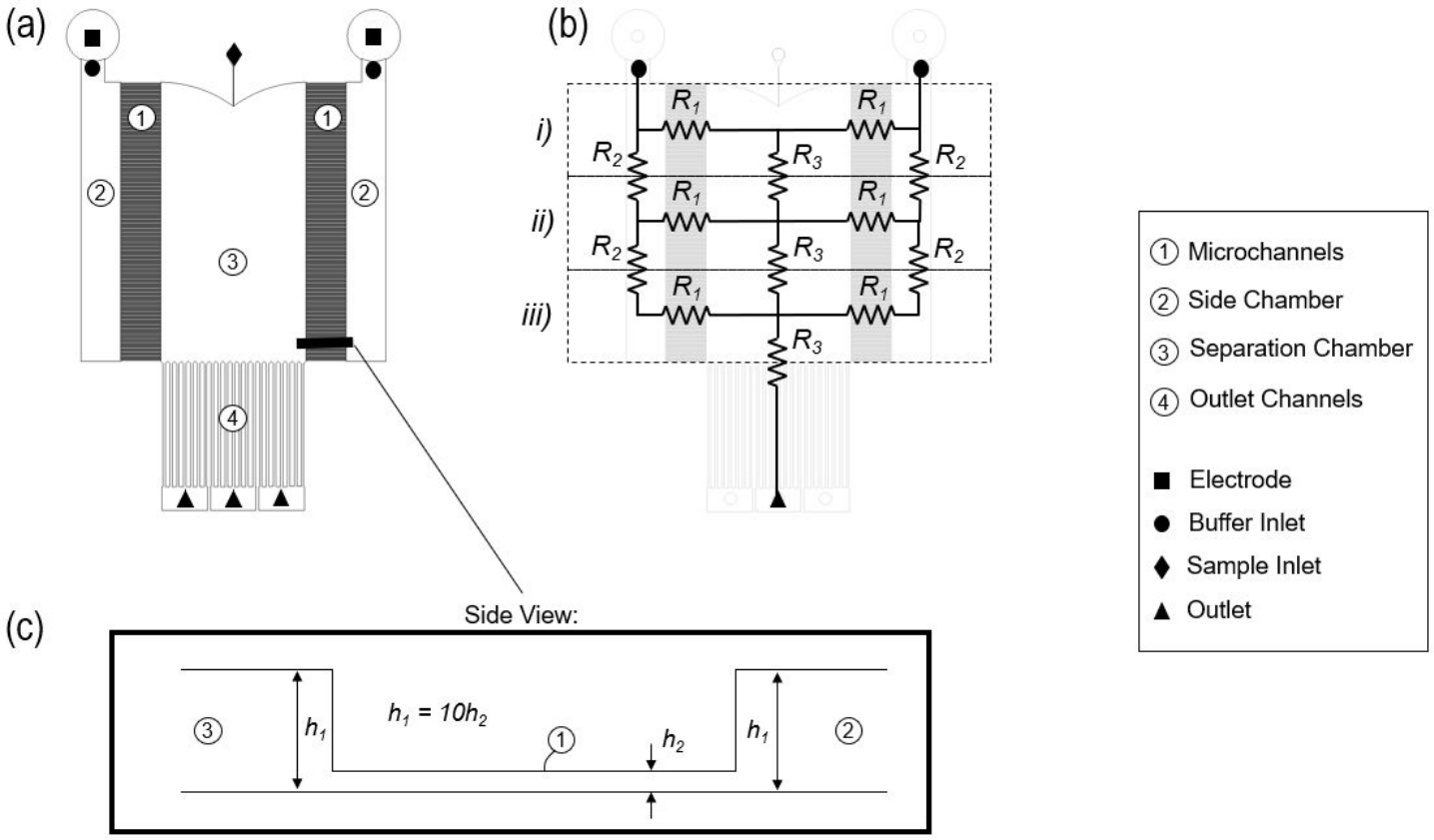

Figure S3. (a) A drawing of a FF-CGF device that includes microchannels that connect side chambers to the separation chamber. There are also outlet channels that connect the separation chamber to the outlets. (b) The FF-CGF device is divided into an upper (i), middle (ii), and lower (iii) section. The approximate resistors for the microchannels (1), side chambers (2), and separation chamber (3) are drawn in each section. (c) A side view of a microchannel with a height (h_2) that is 10 times smaller than that of the connected chambers (h_1).

$$R_H = \frac{12\mu L}{bh^3}\left[1 - \frac{h}{b}\left(\frac{192}{\pi^2}\sum_{n=1,3,5}^{\infty}\frac{1}{n^5}\tanh\left(\frac{n\pi b}{2h}\right)\right)\right]^{-1} \quad \text{(S30)}$$

$$R_E = \frac{L}{\sigma bh} \quad \text{(S31)}$$

where L is the length of the channel, b is the width of the channel, and σ is the conductivity of the fluid [S3]. This is the most effective method for increasing R_H because the h term is cubed in the denominator. The main issue with this strategy is that the microchannels must not be too small, or else the voltage drop across the actual separation chamber will be small.

This problem has been well documented in miniaturized FFE devices that have used microchannels to connect to electrodes [S4]. Therefore, the height ratio between the chambers and the connecting microchannels was limited to 10:1 (see Fig. S3c).

References

[S1] J. C. Giddings, "Crossflow Gradients in Thin Channels for Separation by Hyperlayer FFF, SPLITT Cells, Eiutriation, and Related Methods," *Sep. Sci. Technol.*, vol. 21, no. 8, pp. 831–843, 1986.

[S2] K. Yoo, J. Shim, J. Liu, and P. Dutta, "Mathematical and numerical model to study two-dimensional free flow isoelectric focusing," *Biomicrofluidics*, vol. 8, p. 034111, 2014.

[S3] K. W. Oh, K. Lee, B. Ahn, and E. P. Furlani, "Lab on a Chip Design of pressure-driven microfluidic networks using electric circuit analogy," *Lab Chip*, vol. 12, pp. 515–545, 2012.

[S4] P. Novo and D. Janasek, "Current advances and challenges in microfluidic free-flow electrophoresis—A critical review," *Anal. Chim. Acta*, vol. 991, pp. 9–29, 2017.